BAU Journal - Science and Technology

Volume 4 | Issue 2
ISSN: 2959-331X

Article 2

June 2023

SIZE EFFECT ON THE OPTICAL RESPONSE OF CYLINDRICAL PALLADIUM NANOPARTICLES

Salem Marhaba
Department of Physics, Faculty of Science, Beirut Arab University, Lebanon, s.marhaba@bau.edu.lb

Mohammed Khalaf
Department of Physics, Faculty of Science, Beirut Arab University, Lebanon, mkk305@student.bau.edu.lb

Recommended Citation

Marhaba, Salem and Khalaf, Mohammed (2023) "SIZE EFFECT ON THE OPTICAL RESPONSE OF CYLINDRICAL PALLADIUM NANOPARTICLES," *BAU Journal - Science and Technology*: Vol. 4: Iss. 2, Article 2.
DOI: https://doi.org/10.54729/2959-331X.1094

1. INTRODUCTION

Over the last few decades, tremendous advances in the way objects are manufactured and manipulated on the nanometer scale have allowed us to delve into a fascinating world that could not be reached before, the nano-world. This led to the development of an emerging and rapidly growing research field called plasmonics.

Plasmonics is a field of research concerned with light-matter interactions (Maier, 2007, Marhaba *et al.* 2009). These interactions are very significant in the case of metal nanoparticles (NPs) at a scale near or below the wavelength of light due to the localized surface plasmon resonance (LSPR) optical phenomenon (Trügler, 2016). LSPRs are optical modes supported by metallic nanoparticles due to the negative real part of the complex relative permittivity. This leads to light confinement at the nanoscale causing nearfield local field enhancement inside and outside the metal nanoparticles when excited by illuminating their curved surfaces directly with electromagnetic waves (Maier, 2007, Sherry *et. al.*, 2005, Lermé, Bonnet *et. al.* 2008).

This phenomenon urged significant research interest in many applications of metal nanoparticles such as chemical and biological sensors, near-field microscopy, surface-enhanced Raman spectroscopy, nonlinear optics, heat-assisted magnetic recording, nano-photonics, cancer detection, and treatment (Maier, 2007, Link and El-Sayed, 2000).

The spectral properties of LSPR (amplitude, spectral position, and width) are very sensitive to the geometrical shape, dimensional size, composition of the nanostructure, and the local environment of the nanoparticle (Baida *et al*. 2009, Billaud *et al*. 2008). The spectral properties have been extensively investigated upon studying the absorption, scattering, and extinction cross-sections in the case of Nobel metals mainly gold (Au) and silver (Ag) (Marhaba, 2017). Consequently, these studies have been used to the fullest extent to serve the field of plasmonics and its wide applications (Rashidian *et. al.* 2017). Fewer efforts have been spent on the detailed analysis of Pd transition metal as plasmon nanoparticles although they exhibit some exceptional plasmon properties that are superior to Au or Ag nanoparticles such as index sensitivity, absorption capacity, and wavelength dependence of the dielectric function. In addition, Pd exhibits high stability at elevated temperatures, making it a better candidate for thermo-plasmonic applications (Uson *et. al.* 2022).

In this study, we aimed to investigate the effect of size on the optical properties (absorption, scattering, and extinction cross-sections) of cylindrical palladium nanoparticles. In addition, the effect of the direction of polarization of the electric field on the optical properties was investigated. This was approached theoretically by solving Maxwell's equations for a range of wavelengths of an incident electromagnetic wave (UV-visible-IR regions) to obtain the electric fields and the desired cross-sections. The analytical exact solutions of Maxwell's equations is limited to spherical and isolated nanoparticles only (Grand and Ru, 2019, Lermé, Bachelier *et. al.* 2008, Monk, 2003). In the case of nanoparticles having morphologies as cylinder, cube, cone, … (Amendola *et al.* 2010, Nehl *et al.* 2006), arrangements as dimer, trimer, chain, … (El Samad and Marhaba, 2022, Marhaba and El Samad, 2020) or array of nanoparticles (Marhaba, 2015), the finite element method (FEM) was used to get the solutions in the frame of COMSOL MULTIPHYSICS simulation program.

2. THEORY AND METHODOLOGY

Based on Maxwell's equation, Mie's theory (Bohren, 1998) provides an exact solution for the scattering and absorption of an electromagnetic wave (EMW) by single and isolated spherical nanoparticles (SNPs). Starting with the particle's diameter, material composition, and dielectric characteristics, this theory yields an analytical approach to obtaining the extinction cross-section of a spherical particle.

For nonspherical geometry, as in the case of cylindrical nanoparticles (CNPs), the optical properties (extinction, scattering, and absorption cross-sections) of CNPs can be evaluated by the computation of the electric field during the interaction of the incident electromagnetic wave on their curved surfaces. The electric field is calculated by solving Maxwell's curl equation using Helmholtz wave equations (Grand and Ru, 2019, Marhaba and El Samad, 2021)) defined as:

$$\nabla \times \mu_r^{-1}(\nabla \times \vec{E}) - k_0^2 \left(\epsilon_r - \frac{j\sigma}{\omega\epsilon_0}\right)\vec{E} = 0 \qquad (2.1)$$

where ω, ϵ_0, ϵ_r, σ, $k_{0,}$ and μ_r are the angular frequency, vacuum permittivity, relative permittivity, conductivity, wave number, and relative permeability respectively. Equation (2.1) is solved numerically using COMSOL MULTIPHYSICS simulation program based on the finite element method (FEM). The advantage of this method is that it can compute the optical properties of a nanoparticle of any shape, size or arrangements as mention above.

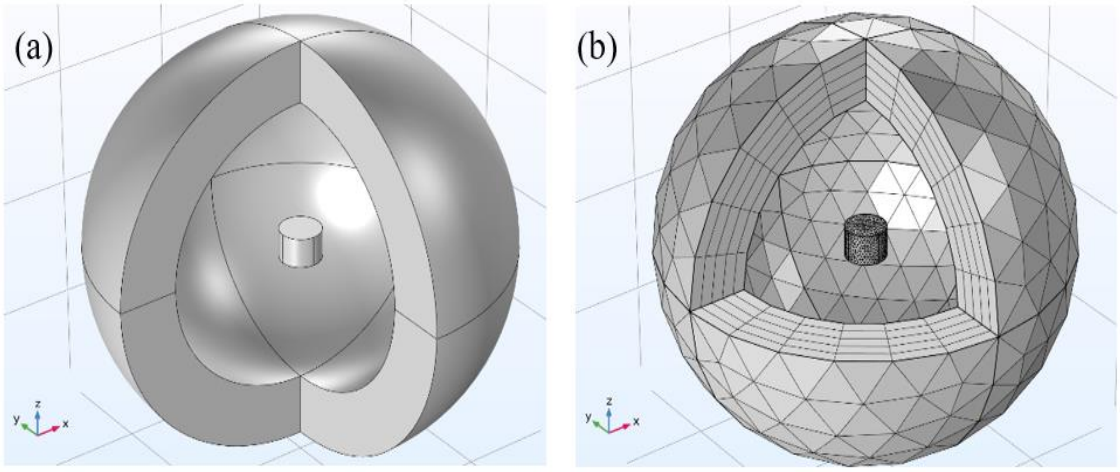

Fig.1: (a) Geometrical model and (b) Meshed model of domain containing CNP of radius $r = 35\ nm$ and height $h = 50\ nm$ suspended in air (refractive index 1).

In the framework of COMSOL, we construct our design by drawing the geometry of the nanoparticle, the surrounding medium, and the perfectly matched layer (PML). In this paper, two different combinations prepare different sizes of the CNPs. The first is changing the radius r of the base of the CNP between 15 nm and 35 nm while keeping a constant height h of 50 nm. The second is changing the height of the CNP between 30 nm and 70 nm while keeping a constant radius of 25 nm. The CNP is centered at the origin and its axis is aligned along the z-direction. (Figure 1).

The CNP is materialized by Palladium (Pd) whose relative permittivity $\varepsilon = \varepsilon_1 + i\varepsilon_2$ are taken from Johnson and Christy (Johnson and Christy, 1974) as shown in figure 2. The values of ε_1 and ε_2 are relevant for plasmonic nanoparticle applications since ε_1 is negative and hence LSPR condition can be satisfied. The real part of the relative permittivity ε_1 is associated with the nanoparticles confining efficiently light at the nanoscale (George *et al.* 2008), while the imaginary part ε_2 is associated with LSPR damping of plasmonic nanoparticle modes (C. Langhammer *et al.* 2007). As observed in the figure 2, the imaginary part of the permittivity is almost uniform and large in the whole range of wavelengths from 200 nm up to 1000 nm. This is due to the overlapping of d-electrons with the s- and p-electrons in the whole range of interest. These values play an important role in the ratios of the contribution of absorption and scattering to the extinction cross-sections of the plasmonic nanoparticles.

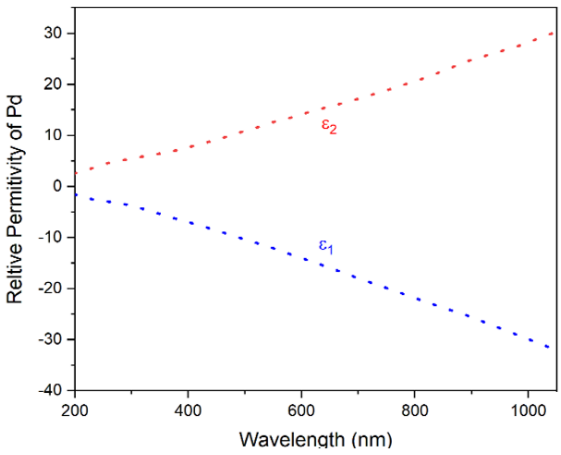

Fig.2: The variation of the real part ε_1 of the relative permittivity and the imaginary part ε_2 as function of wavelength of the incident EMW.

The surrounding medium and the PML are materialized by air with relative permittivity and relative permeability set to 1 while the electric conductivity is set to 0. The PML is an artificial boundary of a truncated region (Figure 1.b) considered a perfect absorbing layer in which incident waves upon the PML do not reflect at the interface (Berenger, 1994). We will consider an incident EMW on the CNP as a background electric field in two orthogonal polarizations. When the EMW is traveling in the z-direction along the axis of the CNP and polarized along the x-direction: $\vec{E} = E_0 e^{\frac{-2\pi i}{\lambda} z}\, \vec{x}$ (Figure 3). When the EMW is traveling in the x-direction perpendicular to the axis of the CNP and polarized along the z-direction: $\vec{E} = E_0 e^{\frac{-2\pi i}{\lambda} x}\, \vec{z}$. Here, $E_0 = 1V/m$ is the amplitude of the electromagnetic field, and λ is the wavelength of the incident EMW ranging between 200 nm and 1000 nm.

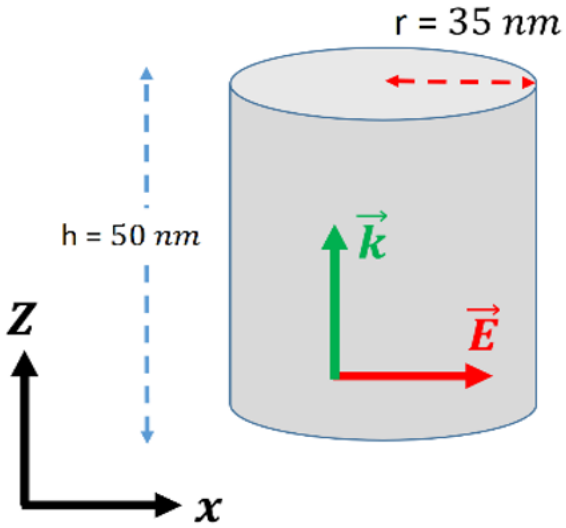

Fig.3: A schematic representation of the direction of travel of the EMW along z- direction aligned with the axis of the CNP as well as the direction of polarization of the electric field along x-direction and perpendicular to the axis of the CNP ($r = 35\ nm$ and height $h = 50\ nm$ suspended in air (refractive index 1)).

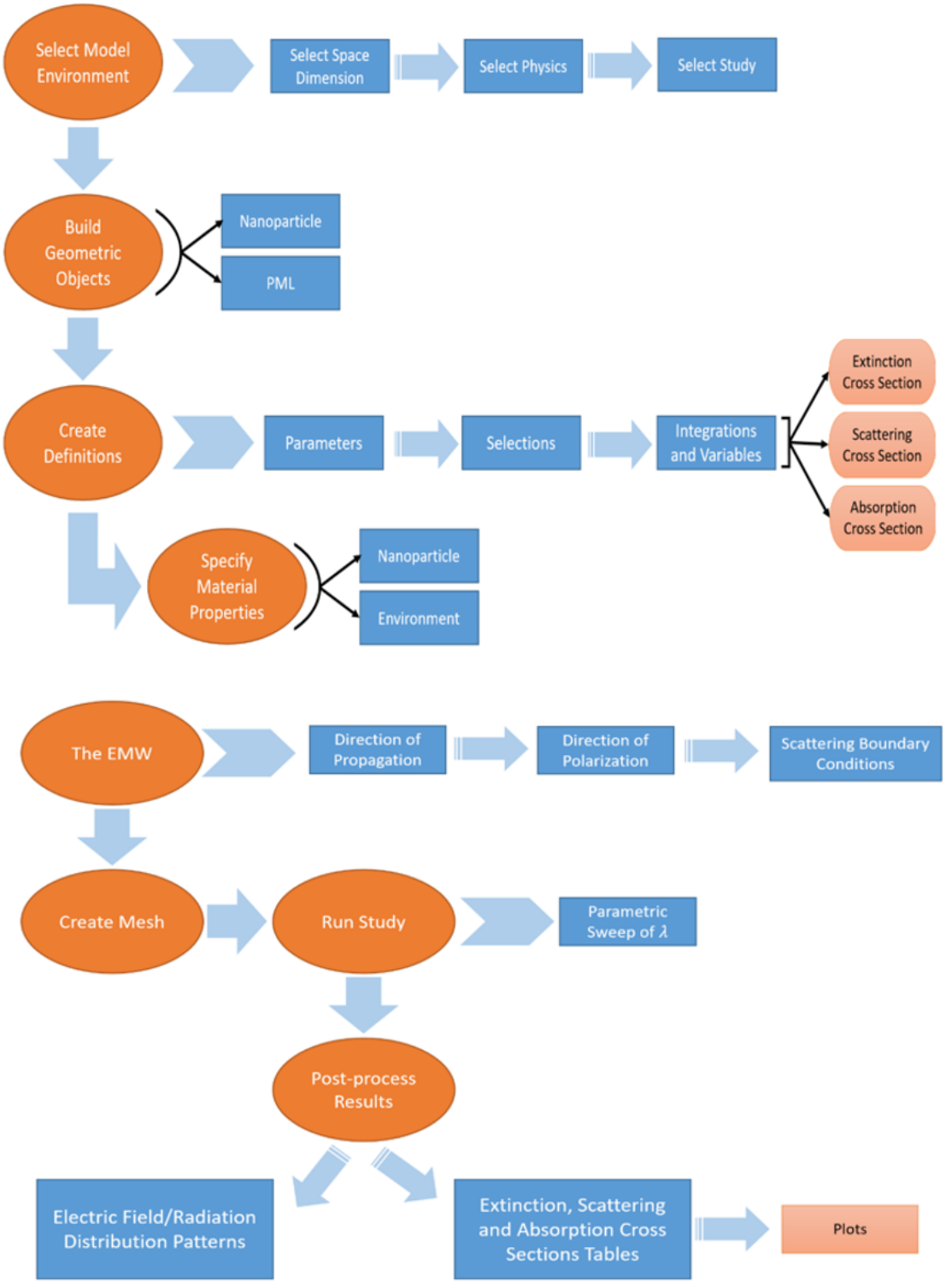

Fig.4: A schematic representation of the COMSOL simulation workflow to describe the methodology used in obtaining the optical properties (absorption, scattering and extinction cross sections) of Pd CNPs.

Meshing the geometry is a crucial step since FEM is based on the discretization of the model into finite elements (Parsons *et al.*, 2010). The free tetrahedral shape is chosen in our model with a maximum element size of $r/6$ for the CNP. The same for the region around the CNP but with a maximum element size of $\lambda/8$. To complete the meshing of the PML, sweeping and distribution techniques are employed with a minimum of 5 layers of discretization of the PML thickness.

(Figure 1. b). After setting all the necessary parameters and variables, COMSOL can solve equation (2.1). The absorption cross-section is calculated from a volume integral inside the NP:

$$\sigma_{\text{abs}} = \frac{1}{S_0} \iiint_{\text{NP}} Q_h dV \qquad (2.2)$$

where $S_0 = {E_0}^2/(2Z_0)$ is the scaling factor, $Z_0 \approx 376.73\ \Omega$ is the impedance of free space, and $Q_h = \frac{1}{2}\omega\epsilon_0 \text{Im}\,(\varepsilon(\omega))|\mathbf{E}(\mathbf{r})|^2$ is the total power dissipation density. $\varepsilon(\omega)$ denotes the relative dielectric function of the particle. The scattering cross section is calculated by integrating the flux of the complex Poynting vector of the scattered field, $\mathbf{S_{sca}}$, across the nanoparticle surface:

$$\sigma_{\text{sca}} = \frac{1}{S_0} \iint_{\text{NP}} \text{Re}\,(\mathbf{S}_{\text{sca}}(\mathbf{r}) \cdot \mathbf{n}) dS \qquad (2.3)$$

The extinction cross-section is obtained from conservation as:

$$\sigma_{\text{ext}} = \sigma_{\text{abs}} + \sigma_{\text{sca}} \qquad (2.4)$$

The obtained data are tabulated automatically and ready to plot. Figure 4 summarizes the COMSOL modelling work.

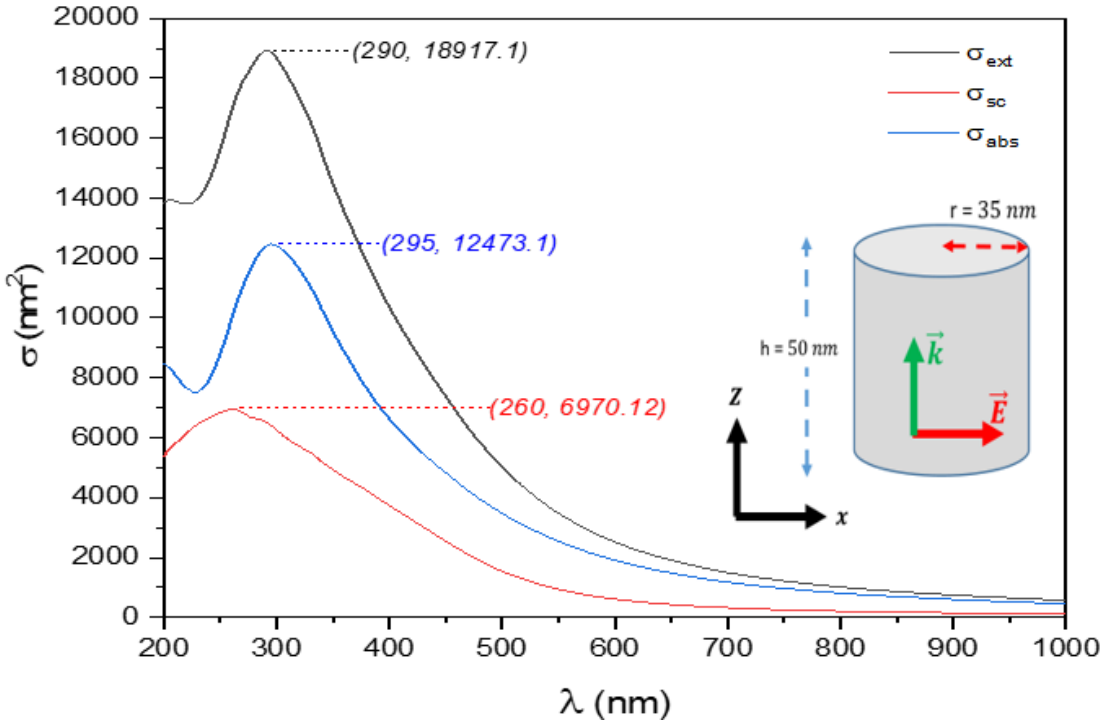

Fig.5: The extinction cross section σ_{ext}, scattering cross section σ_{sc} and absorption cross section σ_{abs} vs. wavelength λ plot for a cylindrical Pd nanoparticle (r=35nm, h=50nm) whose axis is aligned along z-axis and suspended in air (n=1) for polarization parallel to x –axis.

3. RESULTS AND DISCUSSION

The extinction, absorption, and scattering cross sections of a CNP of radius r = 35 nm and height h = 50 nm are shown in figure 5. The axis of the CNP is aligned parallel to the z-axis which is the direction of propagation of the EMW. The EMW is polarized along the x-axis. According to the figure, the LSPR peak positions of scattering, absorption, and extinction are 260 nm, 295 nm, and 290 nm respectively in the near-ultraviolet (NUV) region below the visible one. The amplitude of the absorption cross-section is 12473.1nm^2 slightly less than double that of the scattering cross-section which is 6970.12 nm^2. Since the extinction cross-section is the sum of the absorption and the scattering cross-sections, we can observe that extinction is dominated by absorption. Beyond $\lambda_{LSPR\ peak}$, the wavelength of the LSPR peak, we observe that the three cross sections decrease rapidly in magnitude and become insignificant after crossing the limit of 900 nm. This is predicted due to the high values of the imaginary part ε_2 associated with LSPR damping of plasmonic nanoparticle modes.

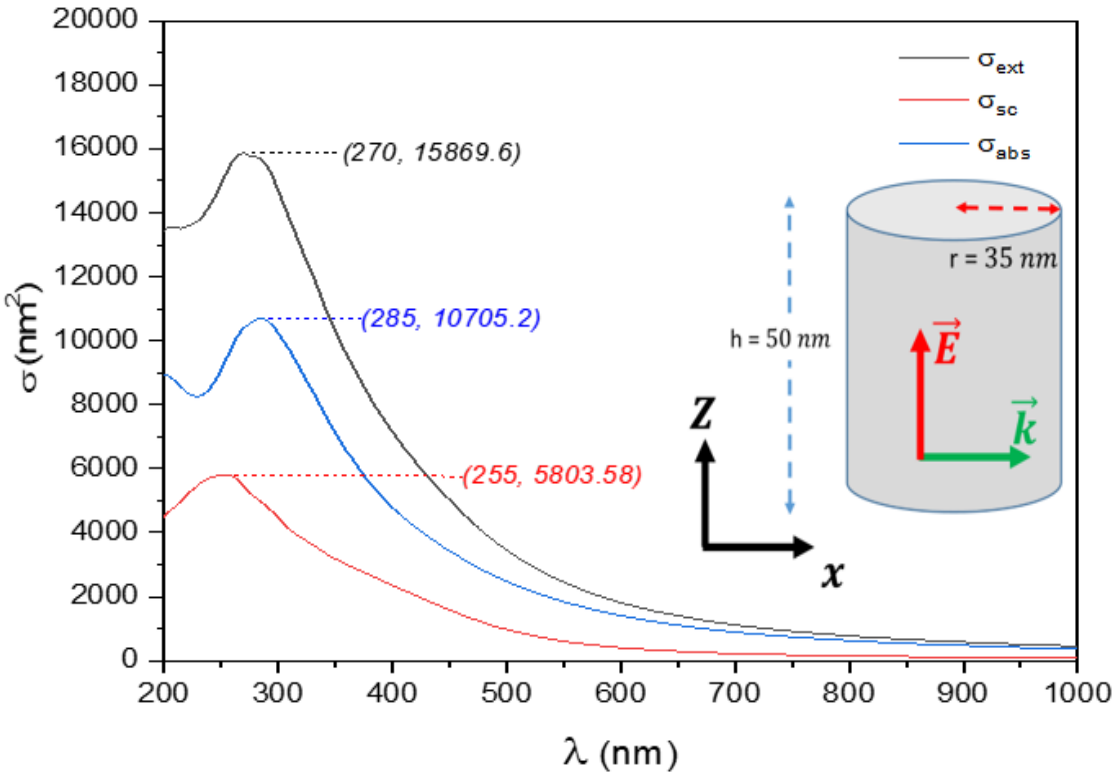

Fig.6: The extinction cross section σ_{ext}, scattering cross section σ_{sc} and absorption cross section σ_{abs} vs. wavelength λ plot for a cylindrical Pd nanoparticle (r=35nm, h=50nm) whose axis is aligned along z-axis and suspended in air (n=1) for polarization parallel to z –axis.

From figure 6, we notice that three plots in the case of z- polarization are very similar in shape to that in the case of x-polarization except that the LSPR peaks blue shift slightly toward lower wavelengths. The amplitudes of the three cross sections decrease noticeably mainly for the absorption cross-section when we change the polarization of the EMW from z-axis to x-axis. In addition, the curve of the extinction cross-section in the case of x-polarization is broader than that in the case of z-polarization (Figure 7). The differences of spectral properties are attributed to the size of the resonating conduction electron gas cloud and its way of oscillation. In the case of z-polarization, the resonating conduction electron cloud is smaller in size compared to that in the case of x-polarization, and hence, the smaller resonator (z-polarization) emits lower wavelengths than the larger resonator (x-polarization). This gives evidence of the importance of the direction of polarization of the EMW for non-spherical nanoparticles.

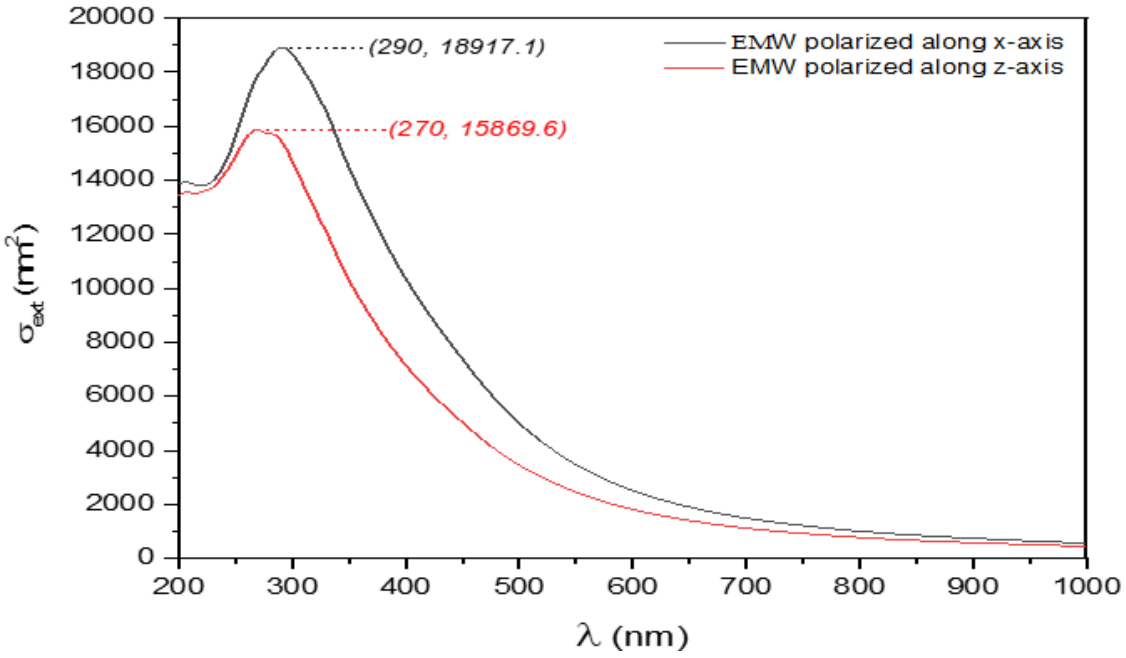

Fig.7: The extinction cross section σ_{ext} vs. wavelength λ plot for a cylindrical Pd nanoparticle (r=35nm, h=50nm) whose axis is aligned along z-axis and suspended in air (n=1) for two different polarizations of EMW: parallel to x-axis and parallel to z-axis.

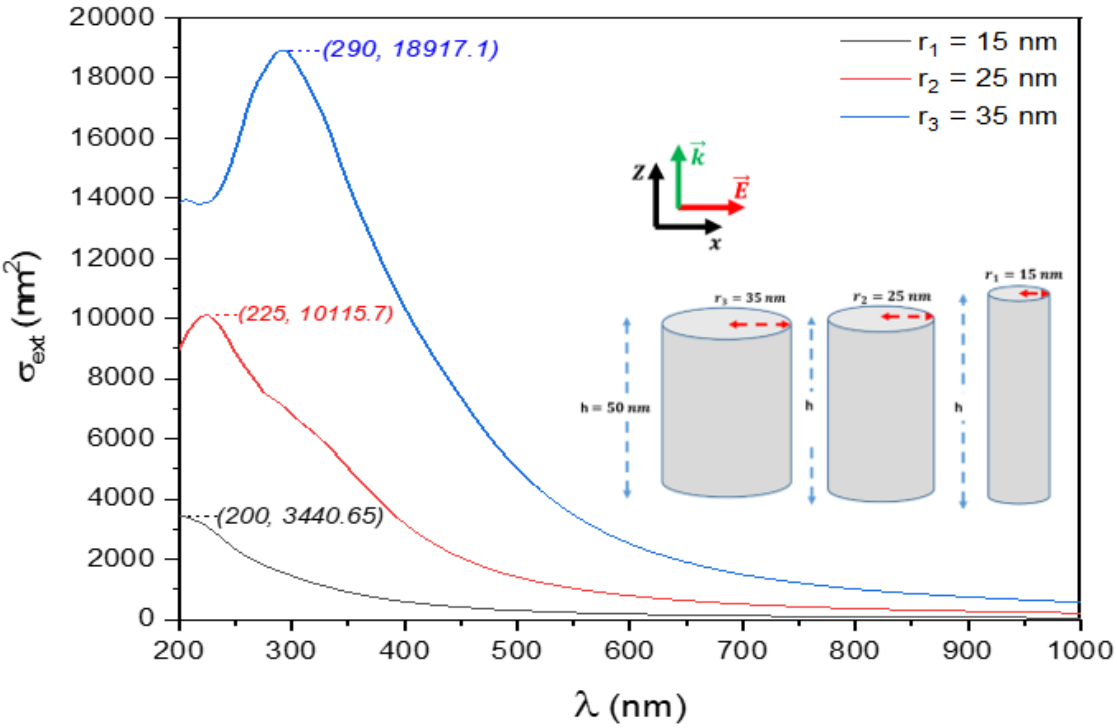

Fig.8: The extinction cross section σ_{ext} vs. wavelength λ plot for cylindrical Pd nanoparticles of same height (h=50nm) but of different radii (15 nm, 25 nm, 35 nm), whose axes are aligned along z-axis and suspended in air (n=1). The EMW is polarized parallel to x- axis in all cases.

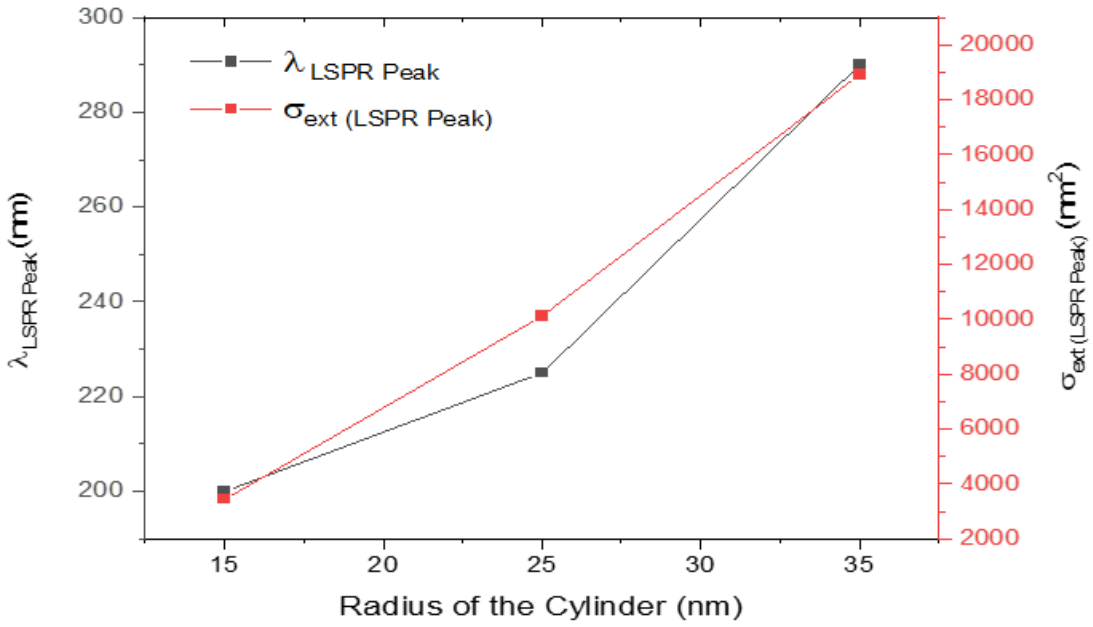

Fig.9: The extinction cross sections and the wavelengths of the localized surface plasmon peaks vs. radius of the CNP

To investigate the effect of size on the optical properties of CNPs, we followed 2 cases.In the first case, three models of CNPs are prepared such that the height is kept constant at h=50 nm, but the radius is varied from 15 nm to 35 nm with a step of 10 nm. The surrounding medium is air with a refractive index of 1. The EMW is traveling in the z-direction while the polarization is parallel to the x-axis. Figure 8 shows the extinction cross-sections for the three models. Based on Figures. 8 and 9, the CNPs underwent a red shift in wavelength with an increase in the radius of the CNPs. The resonance peak for the 15 nm radius was observed at 200 nm. For the 35 nm radius, a resonance peak was observed at 290 nm. The resonance peak shifted by 90 nm, with a change in the CNP radius from 15 to 35 nm. Moreover, Figure 8 shows the effect of CNP radius on the amplitude of the resonance. For a radius of 15 nm, the amplitude of the extinction cross-section was 3440.65 nm^2. This amplitude increases with an increase in CNPs radius and reaches 18917.1 nm^2 when the radius is 35 nm. The resonance amplitude increased by 15476.45 nm^2 with a change in the CNP radius from 15 to 35 nm. Finally, as the radius of the CNPs increases from 15 nm to 35 nm, the curve of the extinction cross-section suffers broadening. Figure 9 shows that as the radius of the CNP increases, a strong redshift is observed with a strong enhancement of the plasmon resonance.

In the second case, three models of CNPs are prepared such that the radius is kept constant at r=25 nm, but the height is varied from 30 nm to 70 nm with a step of 20 nm. Other conditions are maintained the same as in the first case. Figure 10 shows the extinction cross-sections for the new three models. Figure 10 shows that although the height of the CNP is increased from 30 nm to 70 nm, the position of the LSPR peak varies very insignificantly and is almost the same around 225 nm. This is predicted since the direction of polarization of the EMW is parallel to the x-axis where the radius of the CNP is kept constant, so as is the size of the oscillating conduction electron gas. Under these circumstances, the LSPR conditions do not change, and hence the positions of the LSPR peaks do not shift. Similar to the first case, we observe an enhancement by 5174.69 nm^2 in the plasmon resonance as well as a broadening in the extinction spectrum as the height of the CNPs increase from 30 nm to 70 nm.

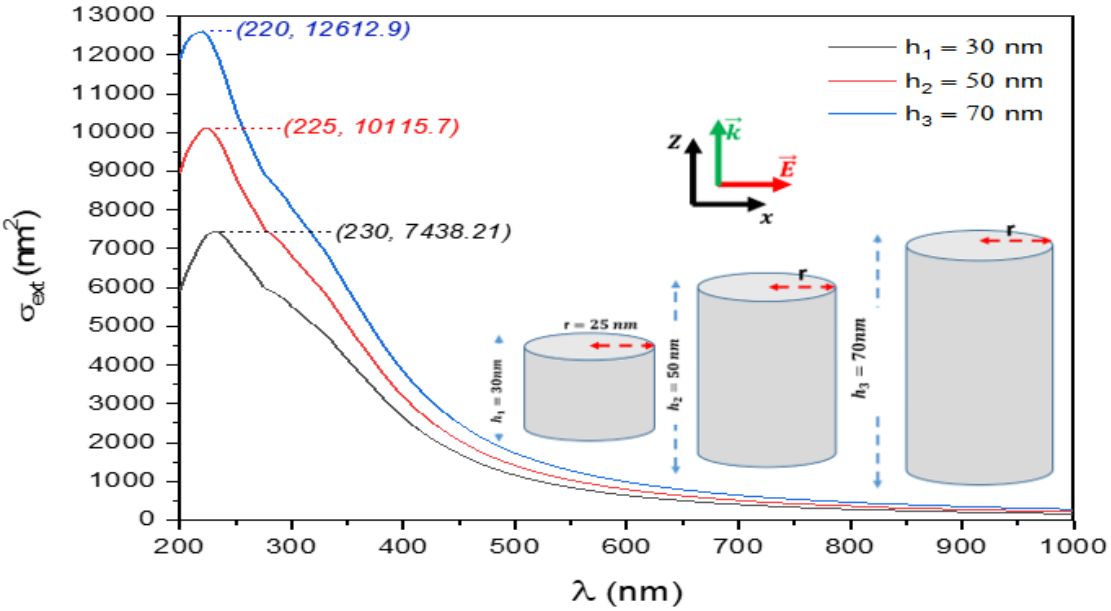

Fig.10: The extinction cross section σ_{ext} vs. wavelength λ plot for cylindrical Pd nanoparticles of same radius (r=25nm) but of different heights (30 nm, 50 nm, 70 nm), whose axes are aligned along z-axis and suspended in air (n=1). The EMW is polarized parallel to x- axis in all cases.

4. CONCLUSION

The optical properties (extinction, absorption, and scattering cross sections) of palladium cylindrical nanoparticles were investigated. They were studied numerically based on the finite element method, where the COMSOL Multiphysics simulation program was employed. The optical properties of palladium nanocylinders were tuned by changing their sizes (radius or height). The resonance peak shifted toward larger wavelengths with an increase in the size of the nanocylinder on the condition that the electromagnetic wave is polarized parallel to the dimension that is increasing. The increase in the size of the nanocylinders yielded a strong redshift, followed by a strong enhancement of the plasmon resonance. The large value of the imaginary part of the relative permittivity of palladium plays an important role in the ratios of the contribution of absorption and scattering to the total extinction cross-sections of the plasmonic nanoparticles. We demonstrated that the extinction cross-section was majorly dominated by absorption rather than by scattering. This property could be useful in thermoplasmonic applications.

REFERENCES

- Amendola, V., Bakr, O. M., & Stellacci, F. (2010). A study of the surface plasmon resonance of silver nanoparticles by the discrete dipole approximation method: effect of shape, size, structure, and assembly. *Plasmonics*, *5*(1), 85-97.
- Baida, H., Billaud, P., Marhaba, S., Christofilos, D., Cottancin, E., Crut, A., & Liz-Marzán, L. M. (2009). Quantitative determination of the size dependence of surface plasmon resonance damping in single Ag@ SiO2 nanoparticles. *Nano letters*, *9*(10), 3463-3469.
- Berenger, J.P., (1994). A perfectly matched layer for the absorption of electromagnetic waves. *Journal of Computational Physics, 114*, 185–200.
- Billaud, P., Marhaba, S., Cottancin, E., Arnaud, L., Bachelier, G., Bonnet, C. & Pellarin, M. (2008). Correlation between the extinction spectrum of a single metal nanoparticle and its electron microscopy image. *The Journal of Physical Chemistry C*, *112*(4), 978-982.
- Bohren, C. F., & Huffman, D. R. (1998). Absorption and scattering of light by small particles, *Wiley-VCH*.
- El Samad, S. & Marhaba, S. (2022). How Light Polarizations Affect the Localized Surface Plasmon Resonance of Asymmetric Palladium Nanostructures. *Nano*, *17*(07), 2250051.
- George, H., Chan, Zhao, J., Schatz, G. C., & Van Duyne, R.P. (2008). Localized surface plasmon resonance spectroscopy of triangular aluminum nanoparticles. *Journal of Physical Chemistry C, 112 (36)*, 13958-13963.

- Grand, J., & Le Ru, E. C. (2019). Practical implementation of accurate finite-element calculations for electromagnetic scattering by nanoparticles. *Springer Science and Business Media LLC. 15*, 109-121.
- Jeon, H. B., Tsalu, P. V. & Ha, J. W. (2019). Shape effect on the refractive index sensitivity at localized surface plasmon resonance inflection points of single gold nanocubes with vertices, *ACS Publications*, 2034–2038.
- Johnson, P. B., & Christy, R. W. (1974). Optical constants of transition metals: Ti, V, Cr, Mn, Fe, Co, Ni, and Pd, *Physical review B, 9*, 5056–5070.
- Langhammera, C., Kasemo, B., & Zorić, I. (2007). Absorption and scattering of light by Pt, Pd, Ag, and Au nanodisks: Absolute cross sections and branching ratios. *The Journal of Chemical Physics, 126*.
- Lermé, J., Bonnet, C., Broyer, M., Cottancin E., Marhaba, S. & Pellarin, M. (2008). Optical response of metal or dielectric nano-objects in strongly convergent light beams. *Physical Review B, 77*(24), 245406.
- Lermé, J., Bachelier, G., Billaud, P., Bonnet, C., Broyer, M., Cottancin, E. & Pellarin, M. (2008). Optical response of a single spherical particle in a tightly focused light beam: application to the spatial modulation spectroscopy technique. *JOSA A, 25*(2), 493-514.
- Link, S., & El-Sayed, M. A. (2010). Shape and size dependence of radiative, non-radiative and photothermal properties of gold nanocrystals. *International Reviews in Physical Chemistry, 19*, 409-453.
- Maier, Stefan A. S. (2006). Plasmonics: fundamentals and applications. *Springer Nature.*
- Manrique-Bedoya, S., Abdul-Moqueet, M., Lopez, P., Gray, T., Disiena, M., Locker, A., Kwee, S., Tang, L., Hood, R.L., Feng, Y. and Large, N. (2020). Multiphysics modeling of plasmonic photothermal heating effects in gold nanoparticles and nanoparticle arrays, *Journal of Physical Chemistry C, 124(31)*, 17172-17182.
- Marhaba, S., Bachelier, G., Bonnet, C., Broyer, M., Cottancin, E., Grillet, N. & Pellarin, M. (2009). Surface plasmon resonance of single gold nanodimers near the conductive contact limit. *The Journal of Physical Chemistry C, 113*(11), 4349-4356.
- Marhaba, S. (2015). Gold nanoparticle arrays spectroscopy: Observation of electrostatic and radiative dipole interactions. *Nano, 10*(01), 1550007.
- Marhaba, S. (2017). Effect of Size, Shape and Environment on the Optical Response of Metallic Nanoparticles. *IntechOpen*.
- Marhaba, S. & El Samad, S. (2020). Plasmonic coupling of one-dimensional palladium nanoparticle Chains. Nano, *15*(05), 2050060.
- Marhaba, S. & El Samad, S. (2021). Interparticle Distance Effect on the Optical Response of Platinum Dimer Nanoparticles. *Chemistry Africa 4* (2), 477-482.
- Monk, P. (2003). Finite element method for Maxwell's equations. *Clarendon Press.*
- Nehl, C. L., Liao, H., & Hafner, J. H. (2006). Optical properties of star-shaped gold nanoparticles. *Nano letters, 6*(4), 683-688.
- Parsons, J., Burrows C.P., Sambles J.R., & Barnes W.L. (2010). A comparison of techniques used to simulate the scattering of electromagnetic radiation by metallic nanostructures. *Journal of Modern Optic, 57*, 356–365.
- Rashidian Vaziri, M.R., Omidvar, A., Shabestari, N.P., & Jaleh, N. (2017). Investigating the extrinsic size effect of palladium and gold spherical nanoparticles. *Optical Materials, 64*, 413-420.
- Sherry, L. J., Chang, S.-H., Schatz, G. C., Van Duyne, R. P., Wiley, B. J., & Xia, Y. (2005). Localized surface plasmon resonance spectroscopy of single silver nanocubes. *ACS Publications, 5*, 2034.
- Trügler, A. (2016). Optical Properties of Metallic Nanoparticles. Springer International Publishing.
- Uson, L., Yus, C., Mendoza, G., Leroy, E., Irusta, S., Alejo, T. & Sebastian, V. (2022). Nanoengineering palladium plasmonic nanosheets inside polymer nanospheres for photothermal therapy and targeted drug delivery. *Advanced Functional Materials, 32*(9).